Individual-Based Modelling of the Development and Transport of a *Karenia mikimotoi* Bloom on the North-West European Continental Shelf

P.A. Gillibrand[1*], B. Siemering[2], P.I. Miller[3] and K. Davidson[2]

[1] Environmental Research Institute, North Highland College, University of the Highlands and Islands, Thurso, KW14 7EE, U.K.

[2] Scottish Association for Marine Science, Scottish Marine Institute, Oban, Argyll, PA37 1QA, U.K.

[3] NEODAAS-Plymouth, Plymouth Marine Laboratory, Prospect Place, Plymouth, PL1 3DH, U.K.

* Corresponding Author
Environmental Research Institute,
North Highland College UHI,
Thurso, KW14 7EE,
U.K.
Tel.: +44 (0)1847 889686
Fax.: +44 (0)1847 889001
Email: philip.gillibrand@uhi.ac.uk

1

Abstract

In 2006, a large and prolonged bloom of the dinoflagellate *Karenia mikimotoi* occurred in Scottish coastal waters, causing extensive mortalities of benthic organisms including annelids and molluscs and some species of fish (Davidson et al., 2009). A coupled hydrodynamic-algal transport model was developed to track the progression of the bloom around the Scottish coast during June – September 2006 and hence investigate the processes controlling the bloom dynamics. Within this individual-based model, cells were capable of growth, mortality and phototaxis and were transported by physical processes of advection and turbulent diffusion, using current velocities extracted from operational simulations of the MRCS ocean circulation model of the North-west European continental shelf. Vertical and horizontal turbulent diffusion of cells are treated using a random walk approach. Comparison of model output with remotely sensed chlorophyll concentrations and cell counts from coastal monitoring stations indicated that it was necessary to include multiple spatially distinct seed populations of *K. mikimotoi* at separate locations on the shelf edge to capture the qualitative pattern of bloom transport and development. We interpret this as indicating that the source population was being transported northwards by the Hebridean slope current from where colonies of *K. mikimotoi* were injected onto the continental shelf by eddies or other transient exchange processes. The model was used to investigate the effects on simulated *K. mikimotoi* transport and dispersal of: 1) the distribution of the initial seed population; 2) algal growth and mortality; 3) water temperature; 4) the vertical movement of particles by diurnal migration and eddy diffusion; 5) the relative role of the shelf edge and coastal currents; 6) the role of wind forcing. The numerical experiments emphasized the requirement for a physiologically based biological model and indicated that improved modelling of future blooms will potentially benefit from better parameterisation of temperature dependence of both growth and mortality and finer spatial and temporal hydrodynamic resolution.

Keywords. *Karenia mikimotoi*, HAB, harmful algal bloom, particle tracking model, coastal waters, bio-physical model.

1.   Introduction

The Scottish west coast and Islands is a region within which harmful phytoplankton are common (Davidson et al., 2011). Most research effort in the region has concentrated on biotoxin producing species of *Alexandrium* (Collins et al., 2009; Touzet et al. 2010; Eckford-Soper et al., 2013), *Pseudo-nitzschia* (Fehling et al., 2004a, 2005, 2006, 2012) or *Dinophysis* (Whyte et al., 2014). Such organisms have had a major economic impact through the closure of offshore scallop fisheries (Campbell et al., 2000; Fehling et al., 2004b), and negative effects on the sustainable development of the rope grown mussel farming industry (Davidson and Bresnan, 2009). A major regulatory monitoring programme is in operation to comply with European Union regulations relating to biotoxin shellfish producing phytoplankton to maintain shellfish safety (Stubbs et al., 2014). However, while the economic value of finfish aquaculture dwarfs shellfish aquaculture in the region, the HAB threat to this sector of the aquaculture industry has received little attention. This is particularly pertinent for what is perceived to be an increasing problem related to the harmful dinoflagellate *Karenia mikimotoi*.

Brand et al. (2012) review the biogeography of different members of the genus *Karenia; Karenia mikimotoi* is one of the most common dinoflagellates in the eastern North Atlantic and has been known to form high density blooms, often clearly visible at the water surface when they are termed 'red tides' or 'brown water' (Dahl and Tangen, 1993). If the cells are of sufficient density, blooms may cause mortality of marine fauna through hypoxia (Tangen, 1977) or the production of haemolytic cytotoxins (e.g. Turner et al., 1987; Satake et al., 2002, 2005). The detailed biology of *K. mikimotoi* is reviewed by Gentien (1998).

Previously known as *Gyrodinium aureolum*, *Gyrodinium mikimotoi* and variations thereof, *K. mikimotoi* has regularly been identified in Scottish waters. Cell densities up to five thousand cells per litre are common, typically with few environmental consequences. However, on a number of occasions, large damaging blooms of *K. mikimotoi* have occurred, the first recorded incidence being in 1980, when cell densities up to 20 million cells per litre were associated with farmed fish deaths (Jones et al., 1982; Roberts et al., 1983). Significant, but again localised blooms were also reported in Orkney and Shetland in 1999 and 2003.

In 2005, a large bloom in the coastal waters west of Ireland caused pelagic and benthic mortalities (Silke et al., 2005), while in 2006, a further large and prolonged bloom of *K. mikimotoi* occurred in coastal waters to the west and north of Scotland (Davidson et al., 2009). As with the Irish bloom, but in contrast to previous Scottish blooms, this event was both temporally sustained and spatially significant. Significant blooms have occurred in many of the years since 2006, with in particular, a large bloom in 2009 in the Firth of Clyde, fortunately to the south of the major finfish aquaculture areas.

Since aquaculture operations are widespread in coastal waters along the Scottish west coast and northern islands (see aquaculture.scotland.gov.uk/map/map.aspx), and are potentially at risk from *K. mikimotoi* blooms, an early warning system of bloom development combined with a capability to predict likely impacted areas is desirable for the industry. Such an early warning system would likely involve remote sensing technology, to identify the seed population, and operational modelling to predict blooms transport and development. The development of remote sensing methodology for *K. mikimotoi* is described by Miller et al. (2006), Shutler et al. (2012) and most recently Kurekin et al. (2014). A complementary component of a forecast system would be a predictive computer model to forecast movements of the developing bloom in the near future. Here, we describe the development of a coupled individual-based bio-physical model that fulfils the second of the above requirements.

Individual-based models (IBMs) are becoming increasingly widely used in marine and fisheries science (Willis, 2011; Davidson, 2014), including harmful algal blooms (Dippner et al., 2011). IBMs use numerical "particles" to represent marine organisms or

clusters of organisms. The particles are typically imbued with aspects of the organism's biology (e.g. growth and mortality) and behavioural characteristics (e.g. vertical migration), and velocity fields extracted from hydrodynamic models are used to advect the particles around the model domain. The IBM approach provides a contrast to that of generic ecosystem models such as ERSEM (Baretta et al., 1995; Allen et al., 2001), which typically model phytoplankton as functional groups and do not resolve to species level, but in which complex interactions between different functional groups and trophic levels may be simulated. Such models are now entering the era of operational forecasting (Siddorn et al., 2007), but forecast modelling of harmful algal blooms using generic ecosystem models is problematic due to the complexity of food web interactions and the difficulty in such a system of discriminating harmful from benign organisms (Allen et al., 2008). For example, Vanhoutte-Brunier et al. (2008) found it necessary to add a specific *K. mikimotoi* algorithm to a generic ecosystem model to study a bloom in the English Channel during 2003.

The IBM presented here is based on the physiological model for the growth and mortality of *K. mikimotoi* derived by Gentien et al. (2007). We coupled that biological model with flow and scalar (i.e. temperature and salinity) fields from the operational deployment (Siddorn et al., 2007) of the Proudman Oceanographic laboratory Coastal Ocean Modelling System (POLCOMS, Holt and James, 2001; Holt et al., 2001). The coupled model was then applied to the simulation of the progression and development of the major *K. mikimotoi* bloom in Scottish coastal waters during the period of July-September 2006. Our approach of coupling IBMs with hydrodynamic flow fields is conceptually similar to that taken for *Alexandrium fundyense* in the Gulf of Maine (Li et al., 2009; Stock et al., 2005) who use cyst surveys in combination with IBM based modelling, to predict potential shellfish toxicity risk in that region.

Water circulation on the continental shelf west of Scotland is dominated by the south-westerly prevailing wind and is strongly influenced by the presence on the continental slope of the North Atlantic (or Hebridean) slope current (Fig. 1). Exchange across the shelf edge between the Atlantic slope current and shelf waters is thought to be sporadic (Huthnance, 1997) but occurs along the length of the Scottish continental shelf boundary (Burrows et al., 1999). Thus an algal bloom appearing on the western Irish coast might be expected to be transported northwards into Scottish waters. On the shelf, the Scottish Coastal Current (SCC) is a predominantly northwards non-tidal flow along the Scottish west coast (e.g. Simpson and Hill, 1986; Hill and Simpson, 1988), but its progress may be moderated by reversals in wind direction and by density effects. The transit time for a parcel of water to be transported by the SCC from the North Channel to Cape Wrath has been estimated from radiocaesium distributions to be six months (McKay et al., 1986). By using the exceptional 2006 bloom as a test case, this paper attempts to understand how these different hydrodynamic and meteorological mechanisms combine with *K. mikimotoi* biology to govern cell transport on the Scottish shelf. Such understanding will be of value to the development of next generation models (Aleynik et al., this issue) that will potentially be capable of bloom early warning.

2. Methods
2.1 Bloom observations
Satellite evidence (Fig. 2) indicated that a large phytoplankton bloom developed offshore to the west of Scotland or Ireland in June 2006. Coastal monitoring indicated that this bloom was likely dominated by *K. mikimotoi* (Davidson et al., 2009). These authors also speculated that the bloom may have been seeded by a bloom of *K. mikimotoi* in western Irish coastal waters during the previous year (Raine et al., 2005), with the remnants of the original event overwintering on the shelf, in the manner suggested by Raine (2004). This hypothesis is consistent with a *K. mikimotoi* bloom in Norwegian waters in 1988, when a bloom in northern latitudes was thought to have been seeded by a more southerly bloom the previous year (Dahl and Tangen, 1990).

The waters on the Malin shelf (Fig. 1) to the west of the Islay front, where the 2006 bloom was first detected, are generally stratified during summer (Simpson et al., 1979; Hill et al., 1997), and it might be expected that the 2006 bloom developed near the pycnocline in a manner similar to that previously reported in the Skagerrak (Richardson and Kullenberg, 1987).

K. mikimotoi cell counts were made from samples collected at 35 sites around the Scottish coast (Davidson et al., 2009). Phytoplankton cells were counted in Utermöhl sedimentation chambers following the methodology of Davidson et al. (2009). Elevated *K. mikimotoi* densities in near-shore waters were first evident in the north of the country, in Orkney waters, in the first week of July (Fig. 3). However, this early bloom remained relatively modest in density (peaking at 3×10^3 cells L^{-1}) and declined to low but finite concentrations by mid-July. A second larger and more prolonged increase in *K. mikimotoi* was evident on the Scottish west coast in mid-July, with densities of 5.3×10^3 cell L^{-1} to the west of Mull, and 7.6×10^4 cell L^{-1} west of Lewis on the 17th of the month (Fig. 3). Once close to land, a generally northwards progression of the peak of the bloom up the Scottish west coast was evident, reaching high densities of 1.7×10^6 cell L^{-1} in the Western Isles on the 31st of July. As the cell density declined in early August in the Western Isles, increases occurred in the Orkney and Shetland Isles, and also on the north-east coast at Golspie and Stonehaven during mid-August. This northward progression is generally consistent with cells being transported by the Scottish coastal current (Simpson and Hill, 1986; Hill et al., 1997; Inall et al., 2009) and Fair Isle current (Turrell et al., 1990), which flow in a clockwise direction along the Scottish mainland.

2.2   Hydrodynamic Model

Three-dimensional velocity fields from POLCOMS were used to drive the progression of the 2006 *K. mikimotoi* bloom. Velocity fields were obtained from the operational runs of the Medium Resolution Continental Shelf (MRCS) version of POLCOMS which are performed at the UK National Centre for Ocean Forecasting (www.met-office.gov.uk/research/ncof/mrcs/, Siddorn et al., 2007). The model has a horizontal spatial resolution of 6-7 km and is forced by modelled wind stresses from the UK Meteorological Office Unified Model. Modelled velocity fields at 5 m depth intervals from 0 – 30 m were obtained via the Environmental Systems Science Centre (ESSC) data server 'Godiva'. The velocity fields are daily-mean values and do not include tidal fluctuations. Three-dimensional daily temperature and salinity fields at the same spatial resolution were also acquired; surface layer temperature at key time periods during July – September 2006 are shown in Fig. 4.

The mean circulation at 5 m depth for the period 1st June – 30th September is shown in Fig. 5. Key features predicted by the model include the Scottish Coastal Current flowing northwards to the west of both the mainland and the Outer Hebrides, and the Fair Isle current (Turrell et al., 1990), which flows eastward at 59°N around the north of Orkney and then southward along the east coast of Scotland. The MRCS model has been evaluated by Holt et al. (2005), who compared the modelled residual currents against observations and calculated an RMS error for the modelled speed of 0.06 m s^{-1}. For temperature, Holt et al. (2005) compared the modelled surface fields with advanced high resolution radiometer (AVHRR) satellite data and obtained a surface temperature RMS error of 1.0 °C. The depth-varying RMS error in temperature, calculated against available CTD data from the North Sea Project, was 0.81 °C (Holt et al. (2005). The pre-operational version of the MRCS model was also evaluated by Siddorn et al. (2007), but the data used were largely obtained from the southern North Sea and Celtic Sea and did not extend to the north-western portion of the continental shelf of interest here.

2.3   Algal Transport and Development Model

The velocity fields were linked to a particle tracking model (e.g. Visser, 1997; Ross

and Sharples, 2004), which uses numerical "particles" to represent "clusters" of *K. mikimotoi* cells. The particles were advected by the velocity field and mixed by horizontal and vertical eddy diffusion, simulating the physical transport and dispersion of the cells. Algal growth and mortality are incorporated in the model, as is vertical migration behaviour driven by a positive phototactic response (Gentien et al., 1998).

The mathematical framework of the model follows standard methodology for advection and diffusion of particles (e.g. Ross and Sharples, 2004; Visser, 1997), whereby the location, $X_P^t = X_P^t(x,y,z)$ of particle P at time t, is calculated according to:

$$\frac{\partial X_P}{\partial t} = \left[\vec{U}_P + w_P\right] + V_H + V_Z \tag{1}$$

where $\vec{U}_P(x,y,z)$ is the 3D model velocity vector at the particle location. Particle advection is treated using a fourth-order Runge-Kutta algorithm. Horizontal and vertical eddy diffusion are represented in the model by the "random walk" displacement "velocities" $V_H(x,y)$ and $V_Z(z)$ respectively. The diffusion velocities are given by (Proctor et al., 1994):

$$V_H(x,y) = R\left[\frac{6.K_H}{\Delta t}\right]^{1/2}$$

$$\tag{2}$$

$$V_Z(x,y) = R\left[\frac{6.K_Z}{\Delta t}\right]^{1/2}$$

where R is a real random number (R ∈ [-1, 1]) with zero mean and a uniform distribution, and K_H and K_Z are the horizontal and vertical eddy diffusivities respectively. For the present simulations, we use a small constant eddy diffusivity of $K_H = 1.0$ m^2 s^{-1}. Other, variable, formulations for K_H are possible, but data are lacking to test the validity of resultant values and so, for simplicity, we use a constant value throughout. Because algal cells were confined to the upper mixed layer in the water column (see below), and did not approach the pycnocline in the model simulations, we also used a constant diffusivity ($K_Z = 0.001$ m^2 s^{-1}) in the vertical. Further modelling may permit cells to migrate to greater depths, crossing the pycnocline, in which case a depth-dependent vertical diffusivity will be required and corrective terms applied to Equation (2) (Ross and Sharples, 2004).

Wind stress can act directly on materials floating on the sea surface or in the near-surface layer (Proctor et al., 1994). To allow for possible direct wind action on the algae, the horizontal velocity taken from the MRCS model may be supplemented by an additional term:

$$\vec{U}_P = \vec{U}_P + \delta_W \vec{W}\left(1 - \frac{\log_{10}(z/z_0)}{\log_{10}(z_C/z_0)}\right) \tag{3}$$

where z is the depth of the particle, z_C is an appropriate lengthscale for the depth of wind influence (here $z_C = 30$ m), z_0 is a surface roughness lengthscale ($z_0 = 0.1$ m), and δ_W the Kronecker delta ($\delta_W = 1$ to include direct wind forcing, otherwise $\delta_W = 0$). The wind velocity, $\vec{W}$, was obtained from wind observations at Tiree, Stornoway and Shetland (Fig. 1), with the closest data to particle locations being determined and used each time step. Equation (3) introduces a wind-induced velocity profile that decays with depth, reaching zero at depth z = z_c. Inclusion of direct wind forcing is specified by the user by defining $\delta_W = 1$ in the model parameter file.

In Equation (1), w_P is the vertical swimming speed of the organism. Gentien (1998)

report that *K. mikimotoi* have been observed to migrate vertically in weakly stratified coastal waters as a result of a positive phototaxis. Migration speeds were given as 2.2 m h^{-1}, with the extent of the migration limited to about 30 m. Since migration is stimulated by a positive phototaxis, we apply an upward swimming speed during daylight hours only; at night, cells are subject to advective and diffusive motions only. To simulate this, at every time step each particle is assigned a vertical velocity, w_p, given by:

$$w_p = \begin{cases} 0.0\,mh^{-1} & if\ t_h < 6\ or\ t_h \geq 18 \\ +2.2\,mh^{-1} & if\ 6 \leq t_h < 18 \end{cases} \tag{4}$$

where t_h is the hour of the day ($0 \leq t_h < 24$). If a particle is located at a depth greater than 30 m (typical surface layer thickness on the European continental shelf), then the upward velocity ($w_p = 2.2$ m h^{-1}) is assigned to ensure that particles do not descend to excessive depths.

Gentien et al. (2007) presented equations for modelled phytoplankton growth and mortality. They simulated concentrations of *K. mikimotoi* as a passive tracer in a one-dimensional dynamical model, and their growth and mortality equations have been adapted here. The growth and mortality of cells was expressed by:

$$\frac{\partial C}{\partial t} = \mu(T)C - K\gamma C^2 \tag{5}$$

where C is the cell concentration (cell L^{-1}), K is a constant (K = 5 x 10^{-5} in Gentien et al., 2007), and μ(T) is the growth rate given as a function of water temperature, T, by:

$$\mu = 1.5 \times 10^{-3}T^3 - 0.15T^2 + 2.8775T - 17.25. \tag{6}$$

where μ is in units of divisions per day. This study used the same expression for μ, using daily temperature data from the MRCS model output. Equation (6) leads to a peak growth at a water temperature of 16°C, with growth ceasing at temperatures below 12°C and above 23°C.

The term γ in Equation 5 represents turbulent velocity shear, a function of turbulence dissipation (Gentien et al., 2007). Greater shear increases the encounter rate of individual cells, which then leads to aggregation, increased density and sinking. The current study did not have access to turbulence parameters from the MRCS output and used instead large scale velocity shear as a proxy for small scale turbulent shear i.e.:

$$\gamma = \frac{U_j - U_{j+1}}{\Delta z_j} \tag{7}$$

where U_j is the velocity at depth level j, and Δz is the vertical separation distance (m) between levels j and j+1. In the MRCS model, velocity fields are available at 5 m depth intervals. The value of the constant K in Equation 5 was revised from the Gentien et al. (2007) value to account for the modified parameterisation of γ, using K = 4 x 10^{-8}. Note that our value of K is three orders of magnitude smaller than that used by Gentien et al. (2007) because our model calculates cell concentrations in cells m^{-3} rather than cell L^{-1}.

The mortality term in Equation 5 represents the encounter rate between cells, leading to coagulation and subsequent deposition (Baird & Emsley, 1999; Gentien et

al., 2007). The parameter K 'takes into account the effective cross-section diameter and a scaling factor' (Gentien et al., 2007). Since turbulence parameters were not available to calculate the shear rate, γ, the physical manifestation of K in Equation 5 is less clearly defined, and the variable becomes effectively a scaling factor and free parameter. It is important, therefore, to determine the sensitivity of the model to K. We varied K in the range $1\times10^{-8} \leq K \leq 5\times10^{-8}$ and investigated the effect on the predicted maximum cell density and total chlorophyll biomass.

Growth and mortality of *K. mikimotoi* cells were strongly dependent on the chosen value of K. As expected, lower values of K led to greater survival of cells, and, since mortality is dependent on the square of cell density, also greater mortality, although the increased production outweighed the increased mortality. The modelled distributions (not shown) of *K. mikimotoi* over the model domain for the case $K = 1\times10^{-8}$ resulted in much higher concentrations of chlorophyll <u>a</u> than were detected by satellite imagery (Fig. 2). We therefore discount $K = 1\times10^{-8}$ as a realistic value. Over the range $2\times10^{-8} \leq K \leq 5\times10^{-8}$ the model was less sensitive, though the cumulative production over the length of the simulation varies almost by a factor of 3 as a result of the changes in K. The optimum value of K for the present model could lie anywhere within this range, and data are not available to reduce this uncertainty. The results presented in this paper were all produced with a value of $K = 4 \times 10^{-8}$.

2.4   Model Simulations

Each numerical particle represented a cluster of *K. mikimotoi* cells, with an initial concentration of $C = C_0$ cell L^{-1}. The model was initialised from a satellite image of surface chlorophyll <u>a</u> concentration for the week ending 1st July 2006 (Fig. 2). By applying published literature values of *K. mikimotoi* chlorophyll per cell (Jones et al., 1982; Dahl et al., 1987; Vanhoutte-Brunier et al., 2008), we converted the remotely-sensed chlorophyll <u>a</u> concentrations into estimates of cell numbers at each pixel location. The initial number of model particles at each grid point was derived from the observed cell count divided by the initial particle concentration C_0. The model stepped forward in time from 1st July to 30th September 2006 with a time step of 600 seconds. Model predictions of surface cell density and the estimated equivalent surface chlorophyll <u>a</u> concentration throughout the domain were output every 24 hours. Note that microscope based cell counts are primarily from shellfish sites located within the fjordic sea lochs of the Scottish west coast. These fjords and their complex hydrography cannot be resolved by shelf wide fixed grid models such as ours, and hence the counts are used to validate the modelled progression and relative (rather than absolute) magnitude of the bloom.

Experimental simulations were then performed, with the model initialised by setting low levels of cell abundance in discrete areas over the model domain. These numerical experiments were designed to test the hypothesis that the Scottish bloom in 2006 may have been triggered by overwintering cells from the *K. mikimotoi* bloom in Irish waters during 2005, with cells from the earlier bloom having potentially been transported as far north and east as the Orkney Islands in the intervening period, either by the Hebridean slope current or by the continental shelf circulation. These simulations were repeated both with and without vertical migrating behaviour, with a goal of assessing the importance of behaviour to the development and transport of blooms. For completeness, simulations with and without algal growth and mortality processes were performed.

Finally, the sensitivity of the results to wind forcing, water velocity and water temperature was investigated. Typically in most of the simulations, direct wind forcing is included i.e. $\delta_W = 1$ in Equation 3, but simulations were also performed with $\delta_W = 0$ to assess the impact of direct wind action on transport of the bloom (Runs 13 – 16). Note that wind effects are also indirectly incorporated in the model via the MRCS velocity fields. The role of advection in driving the observed bloom development was explored by setting velocity to zero throughout the model domain (U = V = 0); as a result,

modelled cell densities were driven purely by biological processes (Runs 17 – 20). Temperature fields extracted from the hydrodynamic model were modified by ±0.5°C and ±1.0°C to examine the sensitivity of the results to the accuracy of the modelled temperature (Runs 21 – 24). Details of the model simulations, including initialisation and parameter values, are given in Tables 1 and 2.

3.   Results

3.1.   The Effect of Initial Cell Distributions

3.1.1   Run 1: Domain-wide Seed Population

Composite maps of ocean colour do not discriminate between *K. mikimotoi* and other phytoplankton species and, while it is understood that many other planktonic organisms contribute to the ocean colour signal, in the absence of any offshore species data, the simplest initial assumption was that the blooming *K. mikimotoi* population dominated the ocean colour imagery and that the chlorophyll biomass could be converted directly to cell density. The implicit assumption, then, is that the seed *K. mikimotoi* population was present at varying concentrations throughout the model domain. Initial particle distributions for the model simulations were derived from the composite MODIS Aqua ocean colour image for the week 25 June – 1 July 2006 by converting observed remotely sensed chlorophyll concentrations into cell densities as described above.

Based on these initial conditions, simulated cell densities at weekly intervals from 1 July 2006 are presented in Fig. 6 after conversion back to equivalent chlorophyll <u>a</u> biomass. Widespread distribution of *K. mikimotoi* is predicted throughout the model domain. In particular, high cell densities developed in the northern North Sea and high densities were sustained along the west coast of Scotland throughout the simulation. Neither of these predictions were supported by observational data (Fig. 2). The model did predict the development of high densities around Orkney in mid-late July and in Shetland in mid-August but in both locations these high densities were sustained in the model simulation, in contrast to transient peaks observed (Figs. 2 and 3).

3.1.2.   Runs 2 & 3: Multiple-Source Seed Population

Based on analysis of the EO data available, Davidson et al. (2009) hypothesised that the 2006 bloom of *K. mikimotoi* originated in Irish coastal waters and moved northward into Scottish waters transported by coastal currents (see Holt and Proctor, 2008). The Scottish Coastal Current has a mean flow speed of about 10 cm s^{-1} (<u>ca.</u> 9 km day^{-1}) to the west of Mull (Inall et al., 2009), but is generally weaker during summer months due to reduced wind forcing. Numerical experiments were performed with the initial seed population restricted to a small area to the west of Mull, close to the location of the initial bloom spotted on the Malin Shelf. Elsewhere in the model domain, *K. mikimotoi* concentrations were set to zero. The results of this simulation (not shown) demonstrated that *K. mikimotoi* cells from the SW Scottish shelf were not transported to the furthest locations of Orkney, Shetland and Stonehaven within the time scale of the observations, indicating that the coastal current alone could not be responsible for the observed progression of the bloom.

An alternative hypothesis to along-shelf transport is that the *K. mikimotoi* seed population was transported northwards from the Irish shelf in the Hebridean slope current and injected onto the continental shelf at multiple locations. The slope current transports water and associated biota northwards along the continental shelf edge (e.g. Souza et al., 2001), from which transient events transport Atlantic water onto the continental shelf (Burrows et al., 1999; Huthnance, 1997). Residual (non-tidal) velocities in the slope current in summer are typically of the order 15-25 cm s^{-1} (Souza et al., 2001), significantly stronger than current speeds in the Scottish Coastal Current. The EO HAB classifier presented by Davidson et al. (2009) predicted the presence of *K. mikimotoi* in the slope current throughout June 2006, with a possible seed population identified to the west of Orkney during the week 26 June – 1 July 2006 (Davidson et al., 2009). Simulations were therefore performed with seed populations limited to two or three discrete areas at the edge of the continental shelf (Runs 2 and 3, Table 2), designed to test the hypothesis of multiple entry of *K. mikimotoi* cells onto the Scottish shelf.

The results of the simulation with two seed populations are presented in Fig. 7. The

initial seed populations for 1st July were located at two points on the continental shelf: (i) the SW corner of the model domain, and (ii) at the shelf edge west of the Orkney islands (Fig. 7, "01-Jul-2006"). The model predictions exhibited a less extensive development of the *K. mikimotoi* population than for the domain-wide seed population, with the two populations remaining distinct throughout the simulation. The SW source population was transported northwards along the western Scottish coast, with cells arriving at Skye and Wester Ross in August and Cape Wrath by mid-September. This rate of progress is commensurate with measured non-tidal current speeds of a few centimetres per second (Hill and Simpson, 1988; Inall et al., 2009). This idealised seed population did not reproduce the appearance of *K. mikimotoi* at the Harris site.

The northern seed population, meanwhile, moved eastwards towards Orkney and Shetland, with cells reaching Orkney in late July and Shetland in late August. After reaching Orkney, this population then travelled southwards along the east coast of Scotland, reaching Stonehaven in mid-August, as noted by Davidson et al. (2009).

A further simulation with three source locations at (i) the SW corner of the model domain; (ii) at the shelf edge to the west of Lewis; (iii) at the shelf edge between Orkney and Shetland (Fig. 8). This simulation again supports the hypothesis that, in order for the *K. mikimotoi* bloom to be present in Shetland in September, the seed population must have been present at the continental shelf edge to the north of the Scottish mainland in early July. Current speeds in the region were not strong enough during the period to transport cells to Shetland from further south in the time available.

3.1.3   Run 4: Uniform Seed Population

The simulation with a uniform background seed population (*ca.* 50 cells L^{-1}) tested the hypothesis that *K. mikimotoi* cells are present at low levels throughout shelf waters and that bloom development is a response to local environmental conditions, in particular water temperature. In this simulation, the bloom clearly developed from the south (Fig. 9), where waters warmed earliest, and progressed northward as warmer temperatures developed (Fig. 4). The temperature-dependent growth submodel (Equation 6) inhibits growth at temperatures below 12°C, and the later bloom at Shetland for example (Fig. 3), may be related to the delay in the development of sufficiently warm coastal waters in the area for *K. mikimotoi* cells to flourish. Water temperatures at the other sampling locations exceeded 12°C several weeks before *K. mikimotoi* concentrations peaked.

This simulation indicated that, given low level seed populations throughout the domain, *K. mikimotoi* concentrations would have reached levels exceeding 10^5 cells L^{-1} throughout much of the domain in August and September (Fig. 9), equivalent to chlorophyll <u>a</u> concentrations of 1.89 µg chl L^{-1}. This widespread bloom was not evident in the monitoring data (Fig. 3) or the satellite imagery (Fig. 2, and Davidson et al. 2009), suggesting instead that the bloom event was confined to a relatively limited area. It seems unlikely, therefore, that the bloom in 2006 was purely the response of a widespread seed population to increasing water temperatures across the region.

3.2.   The Influence of Cell Biology and Behaviour

The key parameters in the biological model of Gentien et al. (2007) are temperature dependent growth and turbulent velocity dependent shear related mortality. In addition vertical migration of *K. mikimotoi* was included. We tested the model sensitivity to these processes, along with the requirement to include a physiological representation of biological growth.

3.2.1.   Runs 5 – 8: Algal Growth and Mortality

Model simulations that did not include processes of algal growth or mortality demonstrated that the development of the bloom was not due solely to physical processes. Advection by residual and wind-driven circulation, from the initial observed distribution, did not result in the order of magnitude variability in observed cell

concentrations. Including algal growth (and also, necessarily, mortality) in the model was essential to reproduce realistic cell distributions, indicating that the observed cell concentrations were due, at least in part, to ongoing development of the bloom over the summer of 2006. We focus on model predictions from the second week of August, when the bloom was at its most intense in two locations: Orkney and Skye (Figs. 2 and 3). With purely advection driving the progression of the bloom, concentrations throughout the domain in mid-August were much lower than observed (Fig. 10 Row 1, cf. Figs 6 - 8). Some aggregation and dispersal of particles was evident, but the high observed cell densities of the order 10^6 cells L^{-1} over significant areas did not materialise.

3.2.2. Runs 9 – 12: Vertical migration

The inclusion of phototactic vertical migration i.e. an upward only swimming speed, was essential for the model to reproduce high densities of cells during daylight hours. Without an upward swimming speed, cells became evenly distributed throughout the surface layer (here limited to a thickness of 30 m) and predicted densities were much lower (Fig. 10 Row 2). Observations suggest that *K. mikimotoi* do display vertical swimming over a limited depth range (Gentien 1998), and other *Karenia* species have been found to migrate to much greater depths (Liu et al., 2001; Sinclair et al., 2006). Conversely, the inclusion of depth-limited downward swimming activity made little difference to the model results. When downward migration was not included, cells were still rapidly mixed throughout the surface layer by vertical eddy diffusion. A downward migration not limited by depth may have more noticeable influence on the transport and development of the bloom, but there is little evidence to support the notion of active downward swimming and downward migration was not explored here.

3.3   The Role of Physical Forcing
3.3.1. Runs 13 – 16: Wind Forcing

The absence of direct wind action had significant effects on the distributions of *K. mikimotoi* cells (Fig. 10 Row 3). With direct wind forcing excluded, distributions of the algal cells shifted noticeably to the south-west. The prevailing wind in early August was from the south-west, so the direct forcing pushed surface cells north-eastward; in areas with a coastline to the north-east, for example on the Malin Shelf, *K. mikimotoi* cells were pressed against the coast, leading to elevated concentrations (e.g. Fig. 6, 12th August). The combination of onshore winds and a positive phototaxis may well contribute to bloom development in nearshore waters as surface water is trapped against the coast. Including direct wind forcing in the model is important to capture such events. The limited spatial and temporal resolution of the current model makes it necessary to include this wind forcing explicitly; in future, utilising flow fields from hydrodynamic models with finer resolution, both spatially and temporally, may better capture the wind-driven circulation, thereby obviating the need to include wind forcing separately through Equation (3).

3.3.2. Runs 17 – 20: Water Velocity

Vanhoutte-Brunier et al. (2008) argued that the 2003 *K. mikimotoi* bloom occurred largely in response to ideal temperature conditions developing in the English Channel, and that advection played a secondary role. Our modelling suggests that for the 2006 bloom, advection was more important than in 2003: simulations without advection, where the bloom was allowed to develop purely in response to water temperature, failed to reproduce the observed concentrations (Fig. 10).

3.3.3   Runs 21 – 24: Water Temperature

The growth of *K. mikimotoi* is modelled as a function of water temperature (Equation 6), as proposed by Gentien et al. (2007). Further numerical experiments, based on the "Two-location seed population" simulation described above, were

conducted with temperature fields predicted by the hydrodynamic model modified by ±0.5°C and ±1.0°C. The accuracy of the water temperature predicted by the MRCS model falls within this range (Holt et al., 2005), but it is important to understand how small errors in the modelled temperature may affect the predicted development of *K. mikimotoi* blooms. The effects of the modified temperature are presented as a difference from the predicted chlorophyll a fields from Run 2 (Fig. 7).

Modelled temperature significantly affected the maximum predicted cell density at the height of the bloom in mid-August (Fig. 11). As might be expected, warmer temperature fields increased the maximum modelled density, and lower temperatures had the opposite effect. The temperature effect was even more marked on the total biomass of *K. mikimotoi*. At the end of the simulations, the total biomass for the T+1.0°C model was more than three times the initial biomass, compared to twice for the baseline simulation. The simulation with T-1.0°C produced an equivalent 50% drop in biomass. The T±0.5°C simulations produced a weaker biomass effect. In contrast to biomass, maximum cell densities only increased by ~20% for the 1.0°C temperature increase. This is a function of the increased mortality at high cell densities limiting the peak densities that may be attained. The main result of the elevated temperature, therefore, was to increase the spatial size of the bloom by encouraging additional growth outside the bloom focal points, rather than increasing the peak intensity at the centre. Importantly, the relationship between temperature and growth is not linear (c.f. Equation 6) and relatively small changes in water temperature have potentially large impacts on production and algal biomass. With upper ocean temperatures expected to increase over the coming century (by a global average of 0.6 – 2.0°C by 2100, IPCC (2013)), future conditions appear likely to favour increased growth of *K. mikimotoi* cells and potentially larger biomass blooms in the future.

4.   Discussion and Conclusions

Individual-based modelling offers a species-specific approach to modelling harmful algal blooms (Davidson, 2014). This type of model allows us to specify behaviour patterns of cells, including vertical migration, growth and mortality, which may differ between species and to examine the effect of those behaviour patterns on population growth, transport and distribution. Increasing computer power enables enhanced complexity in the biological and behavioural parameterisations included in the model, and also allows more numerical particles to be used, improving the model resolution. Both aspects are important to continued improvement of IBMs (Willis, 2011). Here, we typically used almost 0.5 million particles in the simulations, giving a resolution of 113 cells L^{-1} or 0.0021 µg chl L^{-1} (Table 1). Yet the model completed a three-month simulation in less than than one hour on a single CPU. This efficiency permits multiple numerical experiments to be performed that may not be possible using fully-coupled hydrodynamic-ecosystem models due to the higher computational burden. Furthermore, the biology and behaviour patterns are easily adaptable to other species, provided enough is known of their ecology and behaviour. Finally, the IBM approach does not require discretization of cell distributions on to a numerical grid and model results do not, therefore, suffer from numerical artefacts of excessive diffusion or dispersion.

Our model is currently best described as a tool for better understanding the physical and biological processes governing *K. mikimotoi* transport in Scottish coastal waters rather than as an operational simulation system, primarily because of the uncertainty in the initial distribution of the seed population that arises from a lack of offshore species-specific data. For future operational use of this or other models, remote identification of seed populations in real time will be required. Davidson et al. (2009) report some success in developing a discrimination algorithm to identify *K. mikimotoi* from ocean colour data, with further development by Shutler et al. (2012) and Kurekin et al. (2014). Such remote-sensing based systems are necessary to allow the accurate initiation of operational numerical models.

The model results showed qualitative agreement with the *K. mikimotoi* bloom observed from remote sensing and microscope based enumeration at a number of coastal monitoring stations (Davidson et al., 2009). In particular, the progression of the bloom, from the south-west Scottish shelf around the mainland to the northern and eastern coastlines was successfully reproduced. However, the observed progression of the bloom could only be modelled by assuming multiple discrete locations where the seed population was injected onto the continental shelf from the Atlantic margin. In particular, the timing of the observed bloom at Orkney, Shetland and Stonehaven required a modelled seed population in early July to the north of the Scottish mainland. Exchange between the slope current and the continental shelf is known to occur sporadically over short time scales in response to strong tidal and wind-driven flows around Scotland (e.g. Burrows et al., 1999; Huthnance, 1997). Seeding the population with uniform background densities of *K. mikimotoi* resulted in contemporaneous growth of the population throughout the model domain, which does not correlate with the observed progression of the bloom. Conversely, when the bloom was seeded at the southwest corner of the model domain, consistent with the hypothesis of a seed population in Irish waters transported solely by the coastal circulation, the modelled population at the end of September did not extend beyond the west of Scotland. Our contention, therefore, is that the seed population must have entered Scottish coastal waters by multiple pathways, from the south via the coastal current and further north from within the Hebridean slope current.

In the present simulations, cell growth of *K. mikimotoi* is controlled solely by temperature, and mortality is dependent only on velocity shear and population density. A sensitivity analysis demonstrated, unsurprisingly, dependence of predicted bloom magnitude on the modelled temperature, and the mortality coefficient K. Values of these parameters were obtained from Gentien et al. (2007) and hence confidence in model predictions could be improved through study of Scottish strains of *K. mikimotoi* to generate "local" parameter values. To achieve this, laboratory isolates of "Scottish" *K. mikimotoi* are required, a resource that currently does not exist.

Further development of the model structure would include light limitation of growth, following for example the modelling of *K. brevis* by Milroy et al. (2008). Nutrient deficiency in near-surface temperate coastal waters is a well-known inhibitor of plankton growth (Fehling et al., 2006) and might therefore be another potential model development. However, there is field and laboratory evidence that *Karenia spp.* cells can access nutrients through vertically migrating to deep shelf water (e.g. Liu et al., 2001; Sinclair et al., 2006); this mechanism is cited as the reason for high bloom densities observed in oligotrophic coastal waters (Stumpf et al., 2008). Nutrient concentrations may not, therefore, be a limiting factor in population growth, provided sufficient nutrients are available somewhere within the water column. To include nutrient limitation on the growth of algae would require coupling the IBM to a water quality or ecological model (e.g. Vanhoutte-Brunier et al., 2008), but at the cost of a marked increase in modelling complexity (Davidson, 2014).

In the simulations described here, we proscribed a weak vertical migratory behaviour. A positive phototaxis has been proscribed for *K. mikimotoi* (Horiguchi et al., 1999), with cells responding to daylight by active upward swimming, but not actively descending at night; in the model, cells were subjected to downward motion only as a result of turbulent mixing. A positive phototaxis combats vertical turbulent mixing, maintaining a near-surface presence for cells and ultimately promoting bloom development. In simulations performed with non-phototactic cells, turbulent dispersion of cells inhibited bloom development and resulted in much lower cell densities. These results indicate that phototaxis plays an important role in creating harmful algal bloom conditions.

The ultimate goal of this work is to understand the factors governing the development and transport of high biomass harmful algal blooms of *K. mikimotoi* on the Scottish shelf, as a step towards the development of an operational early warning

system to protect the Scottish finfish aquaculture industry from economic losses. As we have demonstrated here, the present model can be easily coupled to operational hydrodynamic model output and run in rapid response to early warnings of bloom development detected by remote sensing, with 7-day forecasts of bloom transport taking little more than an hour to complete. The hydrodynamics of the Scottish continental shelf were provided by operational model simulations, the results of which have been calibrated against available data (Holt et al., 2005; Siddorn et al., 2007). While qualitative comparisons between model and available data were good, extending the model results into the sheltered inshore waters where aquaculture operations are focussed is more problematic. The spatial resolution of current shelf-wide physical models is greater than the size of many of the sheltered coastal bays along the Scottish coastline; these are therefore not resolved by the model grid. Nor are tidal currents included in the MRCS archive, due to the daily temporal resolution; while we do not consider that to be a significant limitation on the shelf-wide simulations reported here, tidal effects will become increasingly important on local scales and will need to be incorporated. Operational models with finer resolution, both temporally and spatially, than those currently available will benefit ongoing testing of the influence of small scale processes and will allow near-shore simulation. The next generation of UK shelf models (e.g. Holt and Proctor, 2008) and/or unstructured grid models (Aleynik et al., this issue) potentially offer just such necessary resolution. Combined with further refinement of the algal transport model and the *K. mikimotoi*-HAB classification algorithm (Davidson et al., 2009; Shutler et al., 2012; Kurekin et al, 2014), these developments offer the real possibility of an effective operational early warning system for UK shelf waters.

Acknowledgments

References

Aleynik, D., Davidson K., Dale A., this issue. A hydrodynamic model structure suitable for harmful algal bloom modelling in areas of complex topography

Allen, J.I., Blackford, J.C., Holt, J.T., Proctor, R., Ashworth, M., Siddorn, J.R., 2001. A highly spatially resolved ecosystem model for the North West European Continental Shelf. Sarsia, 86, 423-440.

Allen, J.I., Smyth, T.J., Siddorn, J.R., Holt, M., 2008. How well can we forecast high biomass algal bloom events in a eutrophic coastal sea? Harmful Algae, 8, 70-76.

Baretta, J.W., Ebenhöh, W., Ruardij, P., 1995. An overview over the European Regional Sea Ecosystem Model, a complex marine ecosystem model. Neth. J. Sea Res., 33, 233-246.

Baxter, J.M., Boyd, I.L., Cox, M., Donald, A.E., Malcolm, S.J., Miles, H., Miller, B., Moffat, C.F., (Editors), 2011. Scotland's Marine Atlas: Information for the national marine plan. Marine Scotland, Edinburgh. pp. 191

Brand, L., Campbell, L., Bresnan, E., 2012. *Karenia*: the biology and ecology of a toxic genus. Harmful Algae 14, 156-178

Burrows, M., Thorpe, S.A., Meldrum, D.T., 1999. Dispersion over the Hebridean and Shetland shelves and slopes, Cont. Shelf Res., 19, 49-55.

Campbell, D., Kelly, M., Busman, M., Bolch, C., Wiggins, E., Moeller, P., Morton, S., Hess, P., Shumway, S., 2001. Amnesic shellfish poisoning in the king scallop, Pecten maximus, from the west coast of Scotland. Journal of Shellfish Research 20(1), 75-84.

Collins, C., Graham, J., Brown, L., Bresnan, E., Lacaze, J.P., Turrell, E., 2009. Identification and toxicity of *Alexandrium tamarense* (Dinophyceae) in Scottish waters. Journal of Phycology 45(3), 692-703.

Dahl, E., Tangen, K., 1993. 25 Years experience with *Gyrodinium aureolum* in Norwegian Waters. In: Smayda, T.J., Shimizu, Y. (Eds.), Toxic Phytoplankton Blooms in the Sea. Elsevier, Amsterdam, pp. 15-21.

Dahl, E., Tangen, K., 1990. *Gyrodinium aureolum* bloom along the Norwegian coast in 1988. In: Granéli, E., et al. (Eds.), Toxic Marine Phytoplankton. Elsevier, Amsterdam, pp. 123–127.

Dahl, E., Danielssen, D.S., Semb, A., Tangen, K., 1987. Precipitation and run off as a fertilizer to a *Gyrodinium aureolum* Hulbert bloom. Rapp. P.-v. Reun. Cons. Int. Explor. Mer. 187, 66-73.

Davidson K., 2014. The challenges of incorporating realistic simulations of marine protists in biogeochemically based mathematical models. Acta Protozool. 53: 129-138.

Davidson K., Bresnan E., 2009. Shellfish toxicity in UK waters: a threat to human health? Environmental Health, 8, S1-S12.

Davidson K., Tett P., Gowen R.J., 2011 Harmful Algal Blooms. In: *Marine Pollution & Human Health* (Eds Harrison and Hester) Issues in Environmental Science and Technology. RSC publishing. pp 95-127. ISBN 978-1-84973-240-6.

Davidson, K., Miller, P.I., Wilding, T.A., Shutler, J., Bresnan, E., Kennington, K., Swan, S., 2009. A large and prolonged bloom of *Karenia mikimotoi* in Scottish waters in 2006. Harmful Algae, 8, 349-361.

Dippner, J.W., Nguyen-Ngoc, L., Doan-Nhu, H., Subramaniam, A., 2011. A model for the prediction of harmful algae blooms in the Vietnamese upwelling area. Harmful Algae 10, 606-611.

Eckford-Soper, L.K., Davidson, K**.,** Bresnan E., 2013. Identification and quantification of toxic and non-toxic strains of the harmful dinoflagellate *Alexandrium tamarense* using fluorescence *in situ* hybridization and flow cytometry. Limnology and Oceanography Methods 11,540-548

Fehling, J., Davidson, K., Bates, S.S., 2005. Growth dynamics of non-toxic *Pseudo-nitzschia delicatissima* and toxic *P. seriata* (Bacillariophyceae) under simulated spring and summer photoperiods. Harmful Algae 4(4), 763-769.

Fehling, J., Davidson, K., Bolch, C.J., Brand, T., Narayanaswamy, B.E., 2012. The relationship between phytoplankton distribution and water column characteristics in north west European shelf sea waters. PLoS ONE 7(3): e34098. doi:10.1371/journal.pone.0034098.

Fehling, J., Davidson, K., Bolch, C., Tett, P., 2006. Seasonality of *Pseudo-nitzschia* spp.(Bacillariophyceae) in western Scottish waters. Marine Ecology Progress Series 323, 91-105.

Fehling, J., Green, D.H., Davidson, K., Bolch, C.J., Bates, S.S., 2004a. Domoic acid production by *Pseudo-nitzschia seriata* (Bacillariophyceae) in Scottish waters. Journal of Phycology 40(4), 622-630.

Fehling, J., Davidson, K., Bolch, C.J., Bates, S.S., 2004b. Growth and domoic acid production by *Pseudo-nitzschia seriata* (Bacillariophyceae) under phosphate and silicate limitation. Journal of Phycology 40(4), 674-683.

Gentien, P., 1998. Bloom dynamics and ecophysiology of the *Gymnodinium mikimotoi* species complex. In: Physiological Ecology of Harmful Algal Blooms (Eds: Anderson DM., Cembella AD and Hallegraeff GM) NATO ASI series vol G41 pp 155-173., Springer-Verlag.

Gentien, P., Lunven, M., Lazure, P. Youenou, A., Crassous, M.P., 2007. Motility and autotoxicty in *Karenia mikimotoi* (Dinophyceae). Phil. Trans. Roy. Soc. B*., 362*(1487), 1937-1946.

Hill, A.E., Simpson, J.H. 1988. Low-frequency variability of the Scottish coastal current induced by along-shore pressure gradients. Est. Coast. Shelf Sci. 27, 163–180.

Hill., A.E., Horsburgh., K.J., Garvine R.W., Gillibrand P.A., Slesser G., Turrell W.R., Adams R.D., 1997. Observations of a density-driven recirculation of the Scottish Coastal Current in the Minch. Est. Coast. Shelf Sci., 45, 473-484.

Holt, J.T., Allen, J.I., Proctor, R., Gilbert, F., 2005. Error quantification of a high-resolution coupled hydrodynamic–ecosystem coastal–ocean model: Part 1 model overview and assessment of the hydrodynamics. J. Mar. Syst., 57, 167-188.

Holt, J.T., James, I.D., 2001. An s coordinate density evolving model of the northwest European continental shelf 1. Model description and density structure, J. Geophys. Res., 106 (C7), 14015-14034.

Holt., J.T., James., I.D., Jones., J.E., 2001. An s coordinate density evolving model of the northwest European continental shelf 2. Seasonal currents and tides, J. Geophys. Res. 106 (C7), 14035-14053.

Holt, J.T. Proctor, R., 2008. The seasonal circulation and volume transport on the northwest European continental shelf: A fine-resolution model study. J. Geophys. Res., 113 (C6).

Horiguchi, T., Kawai, H., Kubota, M., Takahashi, T. and Watanabe, M., 1999, Phototactic responses of four marine dinoflagellates with different types of eyespot and chloroplast. Phycological Research 47, 101–107.

Huthnance, J.M., 1997. North Sea interaction with the North Atlantic Ocean. Deutsche Hydrographische Zeitschrift 49, 153-162.

Inall, M.E., Gillibrand, P.A., Griffiths, C.R., MacDougal, N., Blackwell, K., 2009. On the Oceanographic Variability of the North-West European Shelf to the West of Scotland. J. Mar. Syst., 77 (3), 210-226.

IPCC, 2013: Climate Change 2013. The Physical Science Basis. Contribution of Working Group I to the Fifth Assessment Report of the Intergovernmental Panel on Climate Change [Stocker, T.F., D. Qin, G.-K. Plattner, M. Tignor, S.K. Allen, J. Boschung, A. Nauels, Y. Xia, V. Bex and P.M. Midgley (eds.)]. Cambridge University Press, Cambridge, United Kingdom and New York, NY, USA, 1535 pp.

Jones, K.J., Ayres, P., Mullock, A.M., Roberts, R.J., 1982. A red tide of *Gyrodinium aureolum* in sea lochs of the firth of clued and associated mortality of pond-reared salmon. J. Mar. Biol. Ass. UK, 62, 771-782.

Kurekin, A.A., Miller, P.I. & Van der Woerd, H.J., 2014. Satellite discrimination of *Karenia mikimotoi* and *Phaeocystis* harmful algal blooms in European coastal waters: Merged classification of ocean colour data. Harmful Algae*, 31, 163-176.

Li, Y., He, R., McGillicuddy, D.J., Anderson, D.M., Keafer, B.A., 2009. Investigation of the 2006 *Alexandrium fundyense* bloom in the Gulf of Maine: In-situ observations and numerical modeling. Continental Shelf Research 29(17), 2069-2082.

Liu, G., Janowitz, G.S., Kamykowski, D., 2001. A biophysical model of population dynamics of the autotrophic dinoflagellate *Gymnodinium breve*. Mar. Ecol. Prog. Ser., 210, 101-124.

McKay, W. A., Baxter, M. S., Ellett, D. J., Meldrum, D. T., 1986. Radiocaesium and circulation patterns west of Scotland. Journal of Environmental Radioactivity, 4, 205-232.

Miller, P.I., Shutler, J.D., Moore, G.F., Groom, S.B., 2006. SeaWiFS discrimination of harmful algal bloom evolution. International Journal of Remote Sensing 27(11), 2287-2301.

Milroy, S.P., Dieterle, D.A., He, R., Kirkpatrick, G.J., Lester, K.M., Steidinger, K.A., Vargo, G.A., Walsh, J.J., Weisberg, R.H., 2008. A three-dimensional biophysical model of *Karenia brevis* dynamics on the west Florida shelf: A look at physical transport and potential zooplankton grazing controls. Cont. Shelf Res., 28, 112-136

Proctor, R., Flather, R.A., Elliott, A.J., 1994. Modelling tides and surface drift in the Arabian Gulf – application to the Gulf oil spill. Cont. Shelf Res., 14, 531-545.

Raine, R., 2004. In: Abstracted in Proceedings of the XI International Conference on Harmful Algal Blooms. Cape Town, p. 216.

Richardson, K., Kullenberg, G., 1987. Physical and biological interactions leading to plankton blooms: A review of *Gyrodinium aureolum* in Scandanavian waters. Rapp. P.-v. Reun. Cons. Int. Explor. Mer., 187,19-26.

Roberts, R.J., Bullock, A.M., Turner, M., Jones K.J., Tett, P., 1983. Mortalities of *Salmo gairdneri* exposed to cultures of *Gyrodinium aureolum*. J. Mar. Biol. Ass. U.K., 63, 741-743.

Ross, O.N., Sharples, J., 2004. Recipe for 1-D Lagrangian particle tracking models in space-varying diffusivity. Limnology and Oceanography: Methods, 2, 289-302.

Satake, M., Shoji, M., Oshima, Y., Naoki, H., Fujita, T., Yasumoto, T., 2002. Gymnocin-A, a cytotoxic polyether from the notorious red tide dinoflagellate, *Gymnodinium mikimotoi*. Tetrahedron Letters, 43, 5829–5832.

Satake, M., Tanaka, Y., Ishikura, Y., Oshima, Y., Naoki, H., Yasumoto T., 2005. Gymnocin-B with the largest contiguous polyether rings from the red tide dinoflagellate, *Karenia* (formerly *Gymnodinium*) *mikimotoi*. Tetrahedron Letters, 46, 3537–3540.

Shutler, J.D., Davidson, K., Miller, P.I., Swan, S.C., Grant, M.G., Bresnan, E., 2012. An adaptive approach to detect high-biomass algal blooms from EO chlorophyll-a data in support of harmful algal bloom monitoring. Rem. Sens. Lett. 3, 101-110.

Siddorn, J.R., Allen, J.I., Blackford, J.C., Gilbert, F.J., Holt, J.T., Holt, M.W., Osborne, J.P., Proctor, R., Mills, D.K., 2007. Modelling the hydrodynamics and ecosystem of the North-West European continental shelf for operational oceanography. J. Mar. Syst., 65, 417-429.

Silke, J., O'Beirn, F., Cronin, M., 2005. *Karenia mikimotoi*: An exceptional dinoflagellate bloom in Western Irish Waters, Summer 2005. Marine Environment and Health Series 21, 44 pp.

Simpson, J.H., Edelsten, D.J., Edwards, A., Morris, N.C.G., Tett, P.B., 1979. The Islay Front: Physical Structure and Phytoplankton Distribution. Est. Coast. Mar. Sci., 9, 713-726.

Simpson, J.H., Hill, A.E., 1986. The Scottish Coastal Current. In: The Role of Freshwater Outflow in Coastal Marine Ecosystems. NATO ASI Series Vol. G7.(Ed: S. Skreslet), Springer-Verlag, pp 195-204.

Sinclair, G.A., Kamykowski, D., Milligan, E., Schaeffer, B., 2006. Nitrate uptake by *Karenia brevis*. I. Influences of prior environmental exposure and biochemical uptake on diel uptake of nitrate. Mar. Ecol. Prog. Ser., 328,117-124.

Souza, A.J., Simpson, J.H., Harikrishnan, M., Malarkey, J., 2001. Flow structure and seasonality in the Hebridean slope current. Oceanologica Acta, 24, S63-S76.

Stock, C.A., McGillicuddy, D.J., Solow, A.R., Anderson, D.M., 2005. Evaluating hypotheses for the initiation and development of *Alexandrium fundyense* blooms in the western Gulf of Maine using a coupled physical- biological model. Deep Sea Research (Part II, Topical Studies in Oceanography) 52(19-21), 2715-2744.

Stubbs, B., Swan, S., Davidson, K.**,** Turner, A., Algoet, M., 2014. Annual report on the results of the biotoxin and phytoplankton official control monitoring programmes for Scotland. www.food.gov.uk/sites/default/files/multimedia/pdfs/annualreport-ecoli-scot.pdf.

Stumpf, R.P., Litaker, R.W., Lanerolle, L., Tester, P.A., 2008. Hydrodynamic accumulation of *Karenia* off the west coast of Florida. Cont. Shelf Res., 28, 189-213.

Swan, S., Davidson, K., 2011. Monitoring programme for the presence of toxin producing plankton in shellfish production areas in Scotland. Food Standards Agency.

Tangen, K., 1977. Blooms of *Gyrodinium aureolum* (Dinophyceae) in north European waters, accompanied by mortality in marine organisms. Sarsia, 63, 123-133.

Touzet, N., Davidson, K., Pete, R., Flanagan, K., McCoy, G.R., Amzil, Z., Maher, M., Chapelle, A., Raine, R., 2010. Co-Occurrence of the West European (Gr. III) and North American (Gr. I) Ribotypes of *Alexandrium tamarense* (Dinophyceae) in Shetland, Scotland. Protist 161(3), 370-384.

Turner, M.F., Bullock, A.M., Tett, P.B., Roberts R.J., 1987. Toxicity of *Gyrodinium*

aureolum: some initial findings. Rapp. P.-v. Cons. int. Explor. Mer., 187, 98-102.

Turrell, W.R., Henderson, E.W., Slesser, G., 1990. Residual transport within the Fair Isle Current during the Autumn Circulation Experiment (ACE). Cont. Shelf Res., 10, 521-543.

Vanhoutte-Brunier, A., Fernand, L., Menesguen, A., Lyons, S., Gohin, F., Cugier, P., 2008. Modelling the *Karenia mikimotoi* bloom that occurred in the English Channel during summer 2003. Ecological Modelling 210, 351-376.

Visser, A.W., 1997. Using random walk models to simulate the vertical distribution of particles in a turbulent water column. Mar. Ecol. Prog. Ser., 158, 275-281.

Whyte, C., Swan, S., Davidson, K., 2014. Changing wind patterns linked to unusually high *Dinophysis* blooms around the coast of the Shetland Islands, Scotland. Harmful Algae 39: 365-373.

Willis, J.K. 2011. Modelling swimming aquatic animals in hydrodynamic models. Ecological Modelling 222, 3869–3887.

Table 1. Typical model parameter settings. In some simulations, the value of *cellpp* was modified in order to keep the number of particles to manageable levels. The upward swimming speed and various switches were variously modified for the sensitivity runs.

Parameter Description	Value
Number of particles	457954
Time step of particle model (s)	600
Start day of simulation (Day 1 = 1 June 2006)	31
Time of start of simulation (hh:mm:ss)	15:00:00
Length of simulation (h)	2208
Output frequency (h)	24
Duration of passive stage (d)	0
Duration of mobile stage (d)	200
Upward swimming speed (SS_{UP}, m h^{-1})	2.2
Downward swimming speed (SS_{dn}, m h^{-1})	0
Maximum depth (m)	30
Cell growth switch (1 = yes, 0 = no)	1
Cell mortality switch (1 = yes, 0 = no)	1
Constant in mortality expression, K	4.0×10^{-8}
Minimum velocity shear (s^{-1})	0.001
Number of cells per virtual particle (*cellpp*)	5.0×10^{12}
Conversion rate (μg-chl cell^{-1})	1.89×10^{-5}
Switch for vertical diffusion (1 = yes, 0 = no)	1
Switch for horizontal diffusion (1 = yes, 0 = no)	1
Switch for wind forcing, δ_W (1 = yes, 0 = no)	1
Cell density resolution (cells L^{-1})	113
Chlorophyll <u>a</u> resolution (μg L^{-1})	0.0021

Table 2. List of numerical experiments. In the right hand column, modified parameter values from those given in Table 1 are shown (upward swimming speed (SS_{UP}), growth/mortality and wind switches). Changes to the water temperature (T) and velocity (U, V) from the hydrodynamic model are also indicated. For the differing seed populations (baseline, two-location, three-location, and uniform), no significant changes were made to the parameter values listed in Table 1.

| Run	Run Description	Modified Value
1	Domain-wide initial seed population from satellite imagery.	None
2	Two-location initial seed population.	None
3	Three-location initial seed population.	None
4	Uniform initial seed population (56 cells L^{-1}).	None
5	Domain-wide seed population. No growth or mortality.	Switches = 0
6	Two-location initial seed population. No growth or mortality.	Switches = 0
7	Three-location initial seed population. No growth or mortality.	Switches = 0
8	Uniform initial seed population. No growth or mortality.	Switches = 0
9	Domain-wide initial seed population. No vertical migration.	$SS_{UP} = 0.0$
10	Two-location initial seed population. No vertical migration.	$SS_{UP} = 0.0$
11	Three-location initial seed population. No vertical migration.	$SS_{UP} = 0.0$
12	Uniform initial seed population. No vertical migration.	$SS_{UP} = 0.0$
13	Domain-wide initial seed population. No wind.	$\delta_W = 0$
14	Two-location initial seed population. No wind.	$\delta_W = 1$
15	Three-location initial seed population. No wind.	$\delta_W = 1$
16	Uniform initial seed population. No wind.	$\delta_W = 1$
17	Domain-wide seed population. Zero velocity.	$U = V = 0$
18	Two-location initial seed population, Zero velocity.	$U = V = 0$
19	Three-location initial seed population. Zero velocity.	$U = V = 0$
20	Uniform initial seed population. Zero velocity.	$U = V = 0$
21	Two-location initial seed population. Temperature - 1.0 °C	$T = T - 1.0$ °C
22	Two-location initial seed population. Temperature - 0.5 °C	$T = T - 0.5$ °C
23	Two-location initial seed population. Temperature + 0.5 °C	$T = T + 0.5$ °C
24	Two-location initial seed population. Temperature + 1.0 °C	$T = T + 1.0$ °C
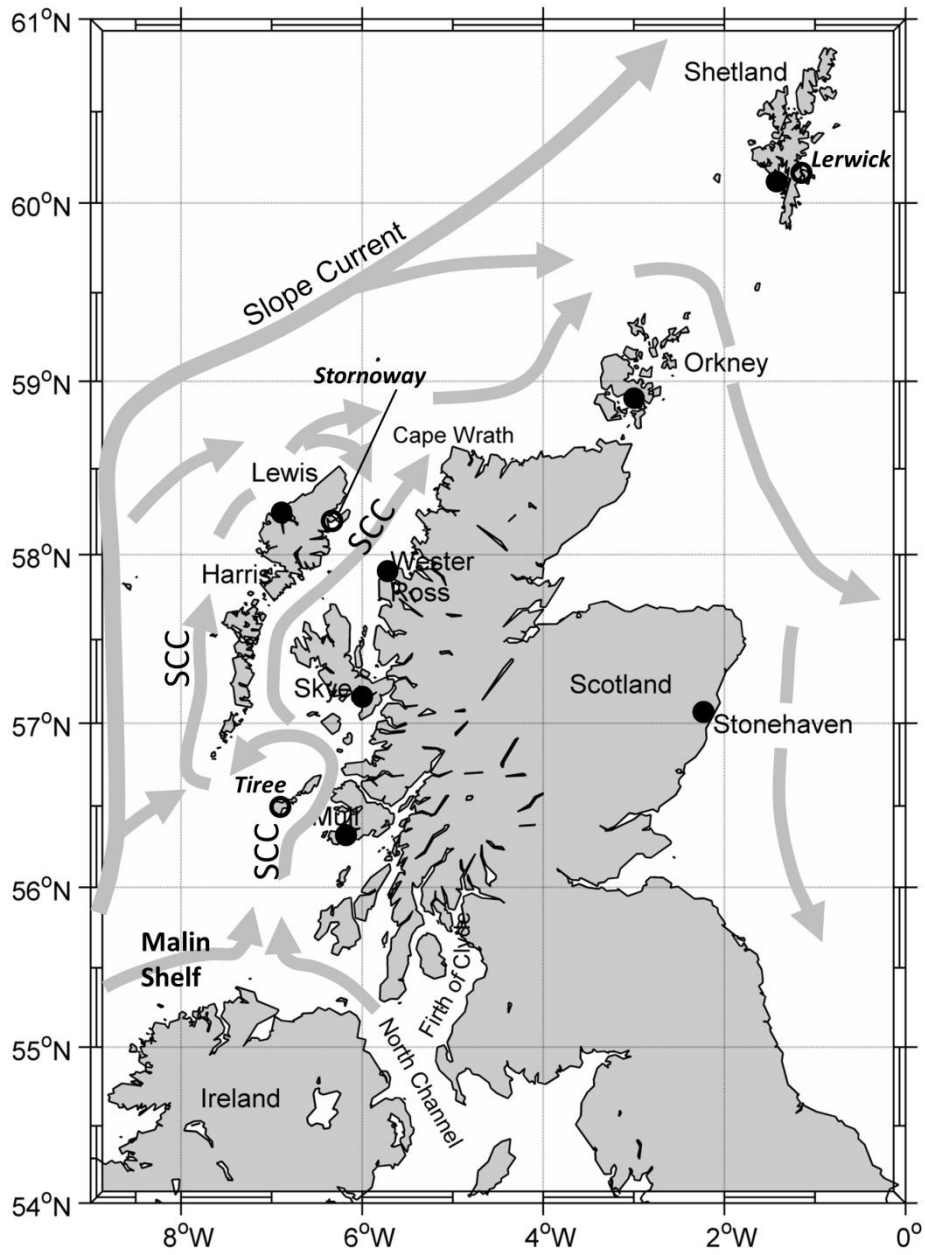
Figure 1. Scottish phytoplankton sampling locations discussed in the text (●) overlain on a schematic representation of the non-tidal water circulation on the Scottish continental slope and shelf (derived from Baxter et al., 2011 and Burrows et al., 1999). The Scottish Coastal Current is indicated by SCC. Wind observation data were obtained from the meteorological stations at Lerwick, Stornoway and Tiree (o).
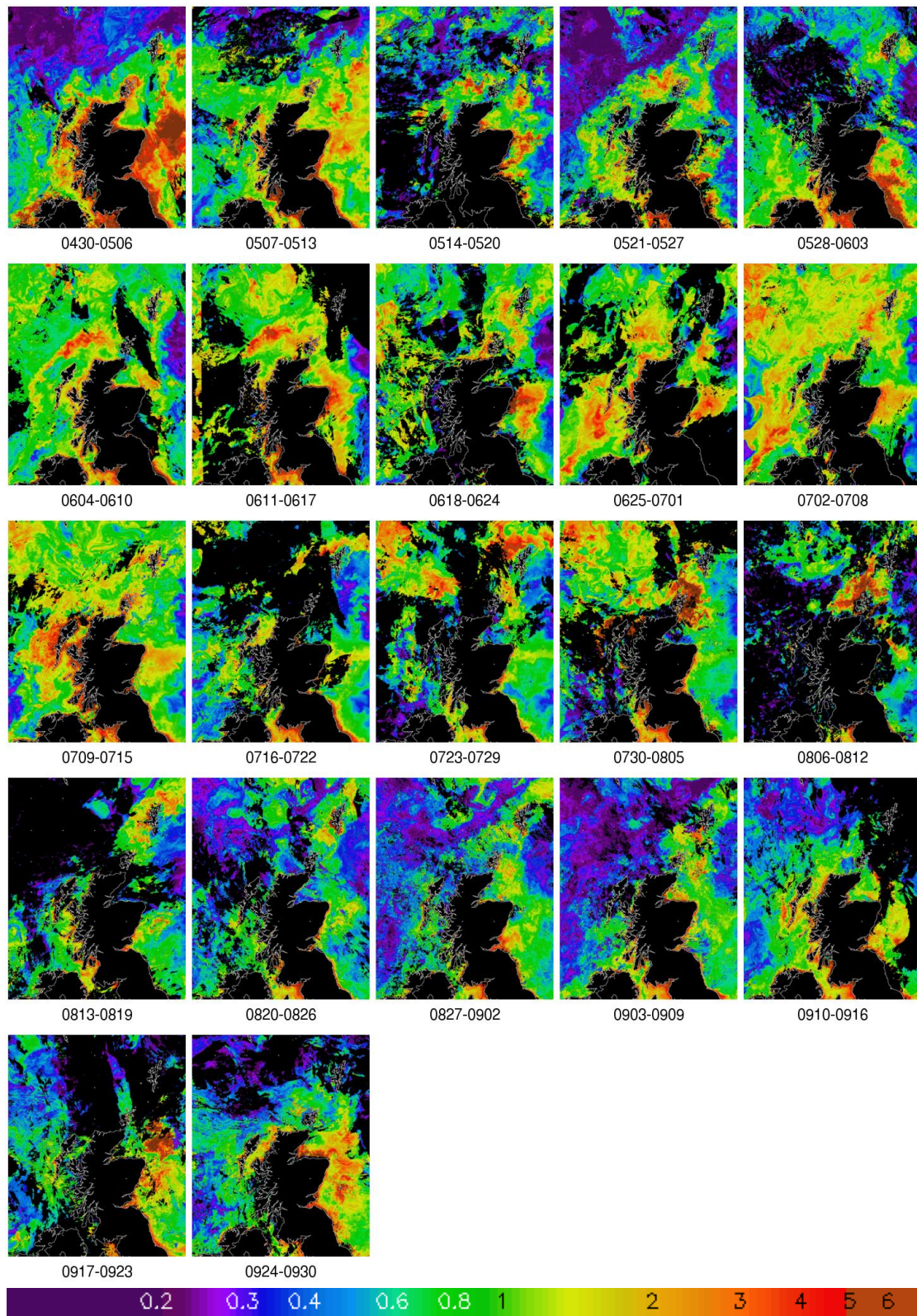
Figure 2. Time-series of MODIS Aqua chlorophyll $\underline{a}$ (μg L^{-1}) weekly median composite maps from May to September 2006. Each weekly map is labelled with the date range (MMDD-MMDD) in 2006.
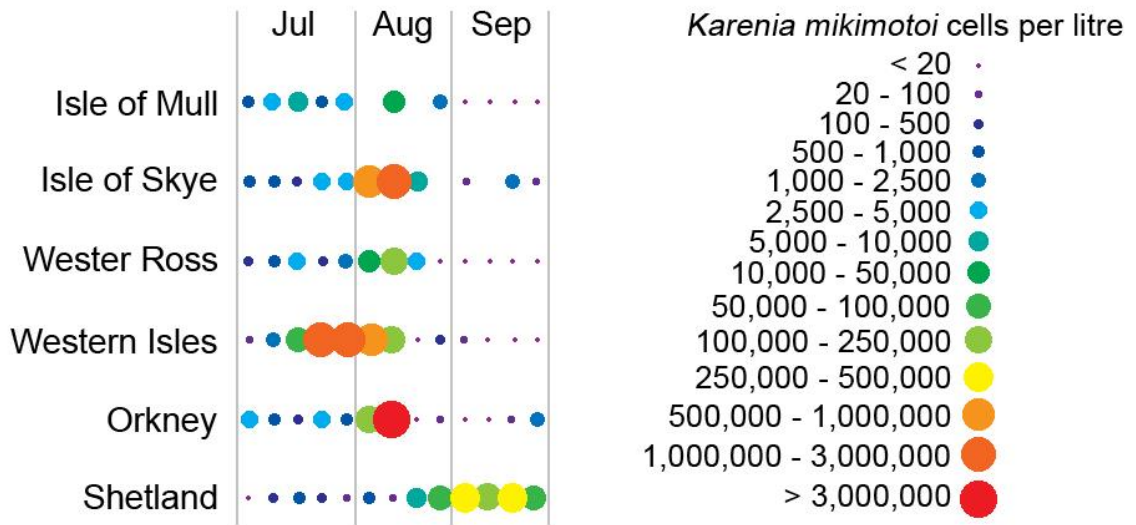
Figure 3. Time series of *K. mikimotoi* cell densities for each region taken from representative coastal monitoring sites (redrawn from Davidson et al., 2009).
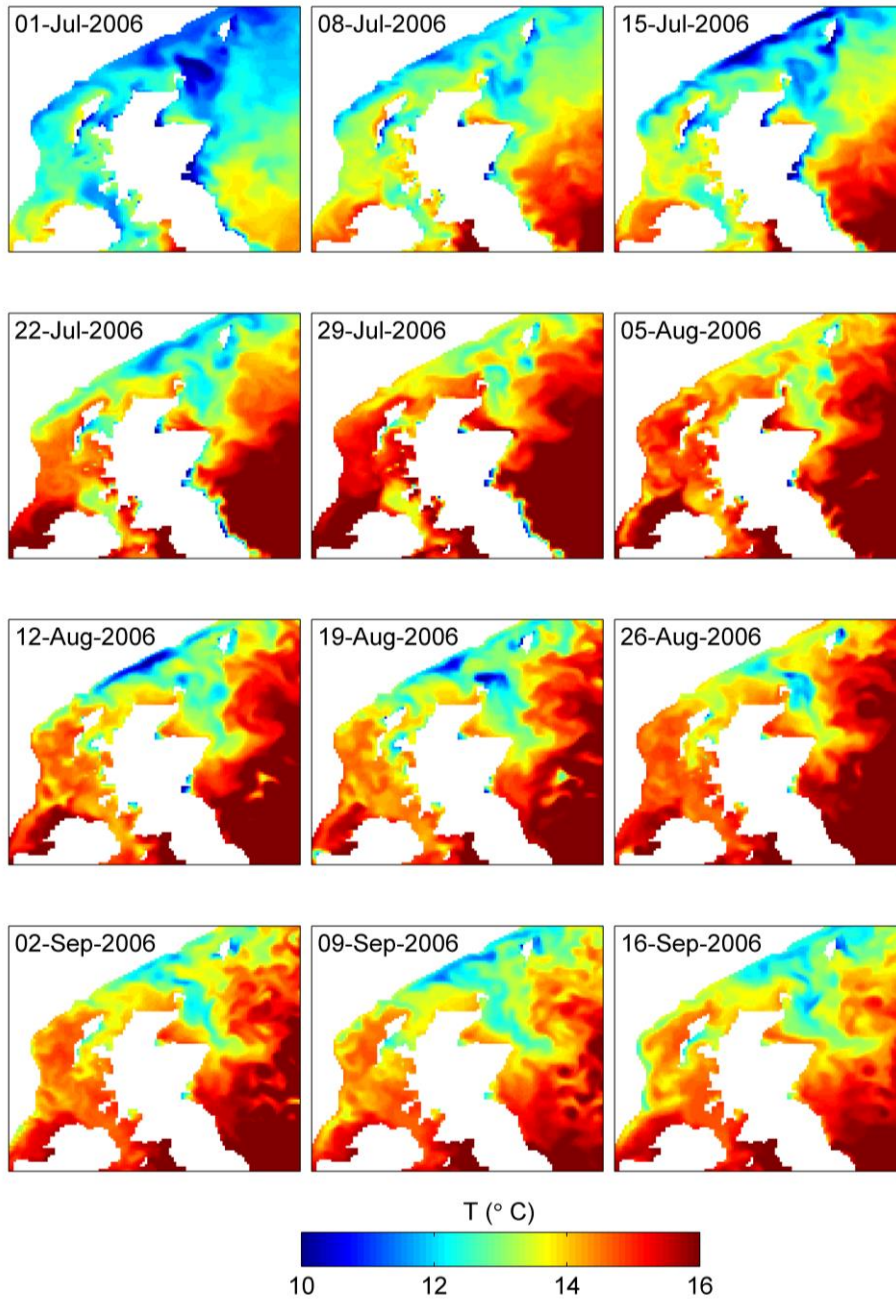
Figure 4. Surface-layer water temperature (°C) at weekly intervals from July – September 2006, taken from the MRCS hydrodynamic model output.
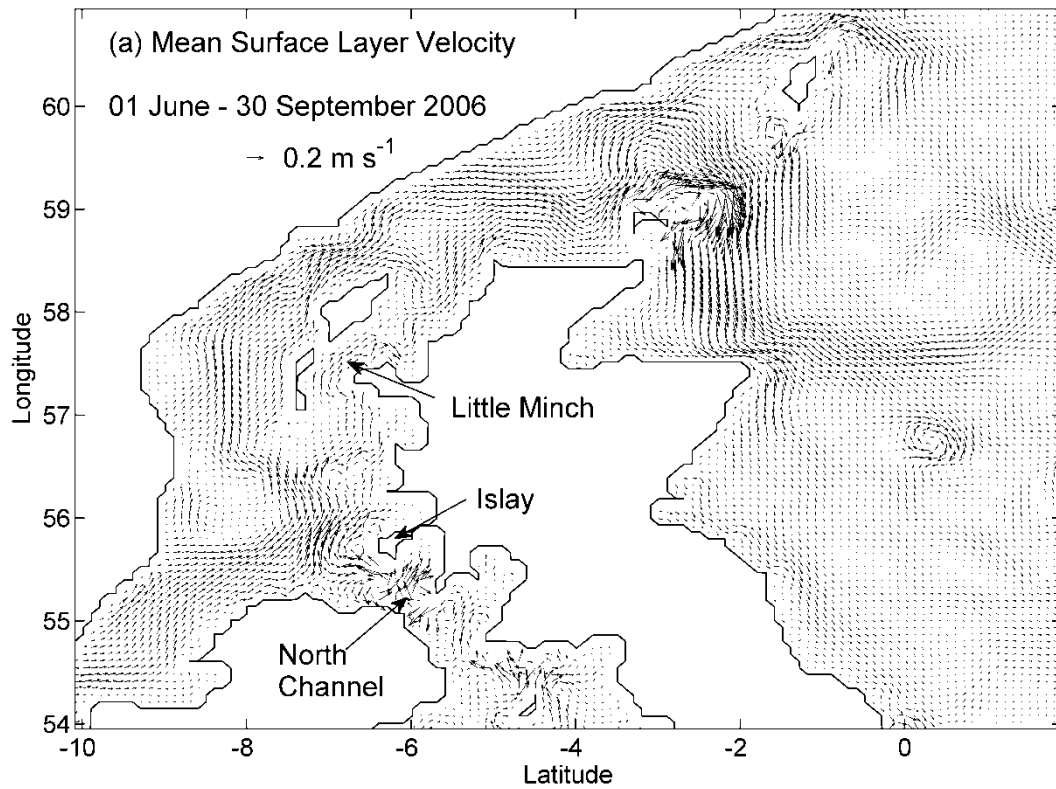
Figure 5. Mean surface layer currents from the operational forecasts by the MRCS model for the period 1 June – 30 September 2006.
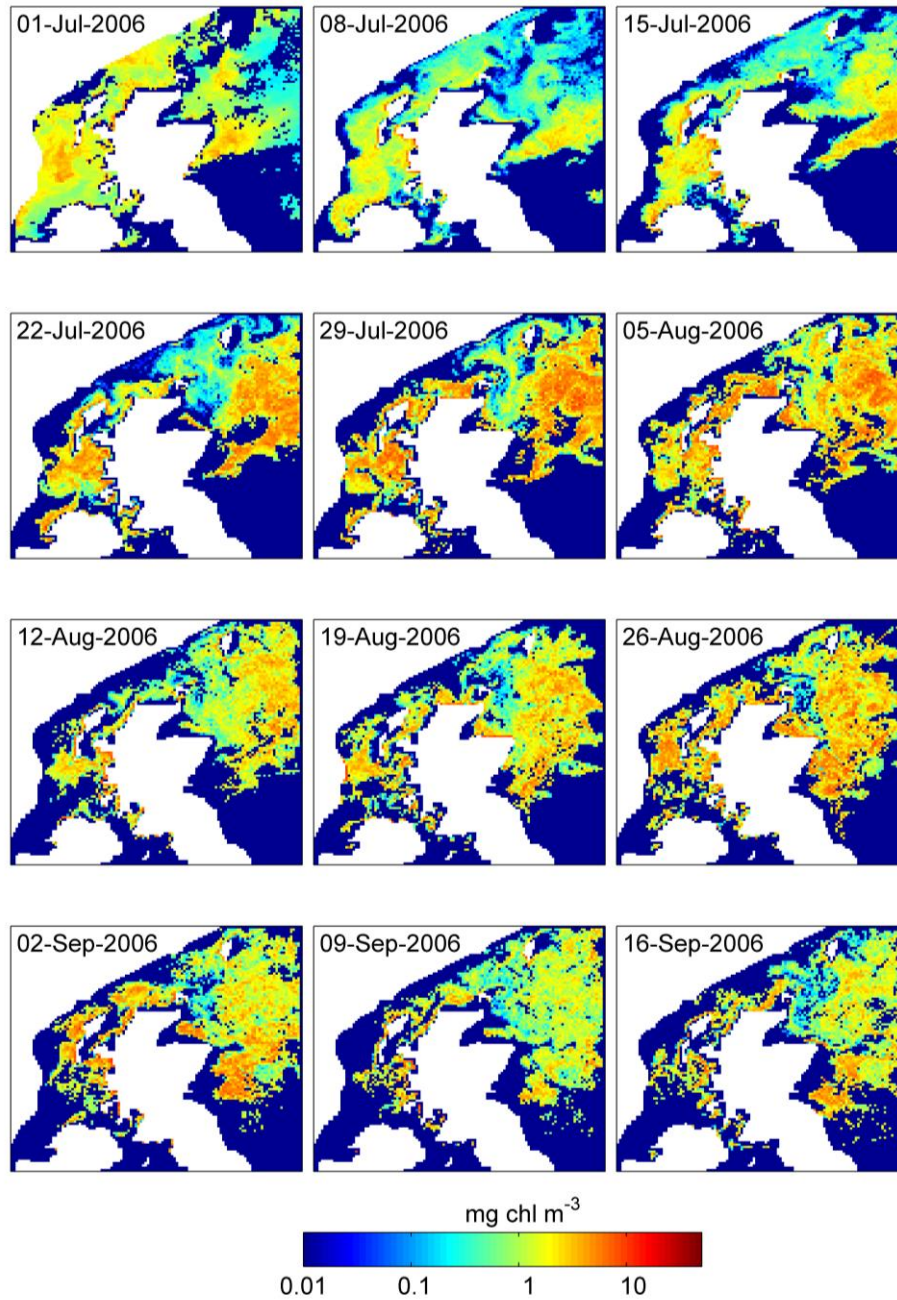
Figure 6. Model-predicted surface concentrations of chlorophyll a (µg L^{-1}), derived from predicted *K. mikimotoi* cell density, at weekly intervals, taken from the domain-wide seed population simulation (§ 3.1.1). Note the high concentrations around Orkney and Skye in early August.
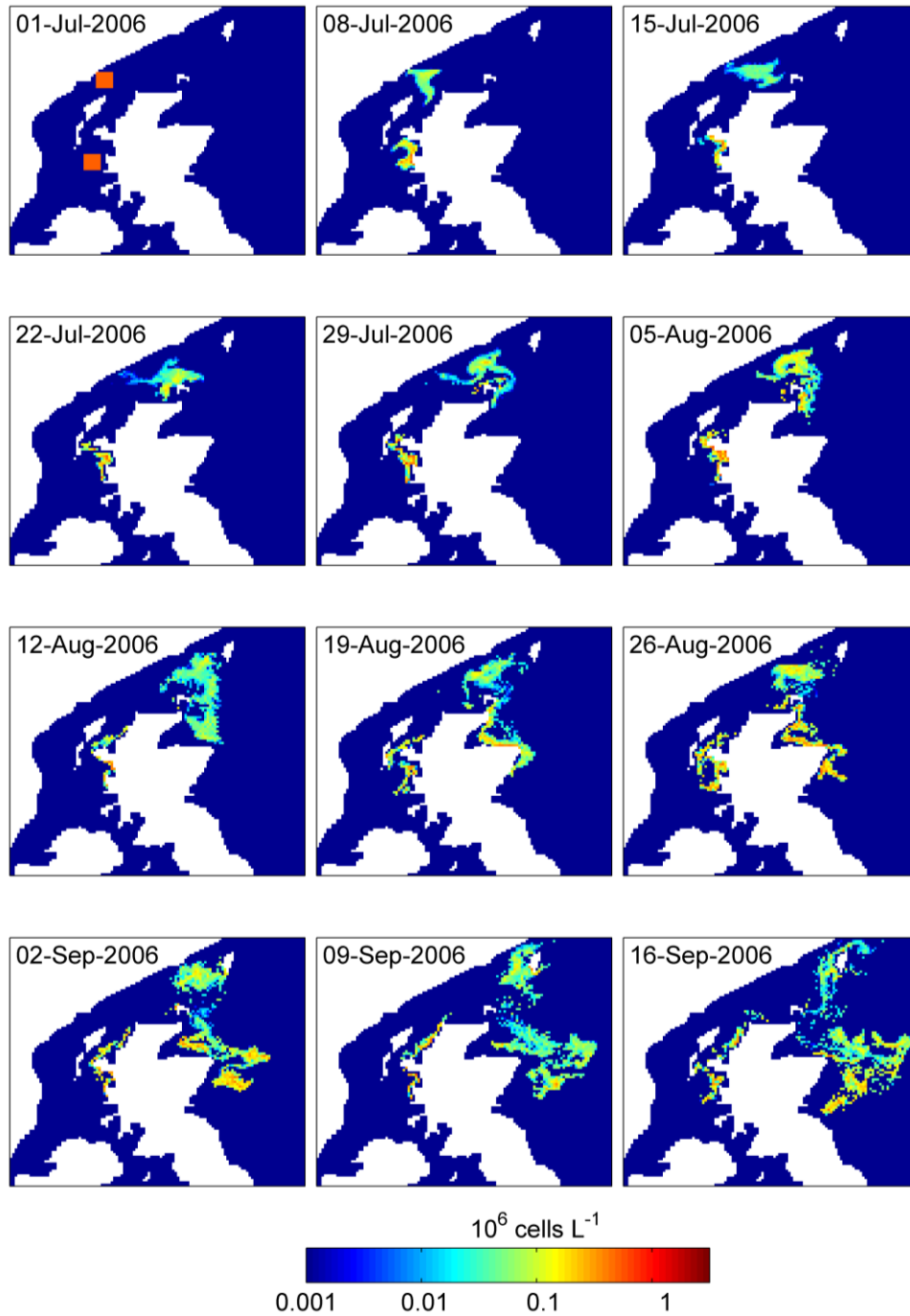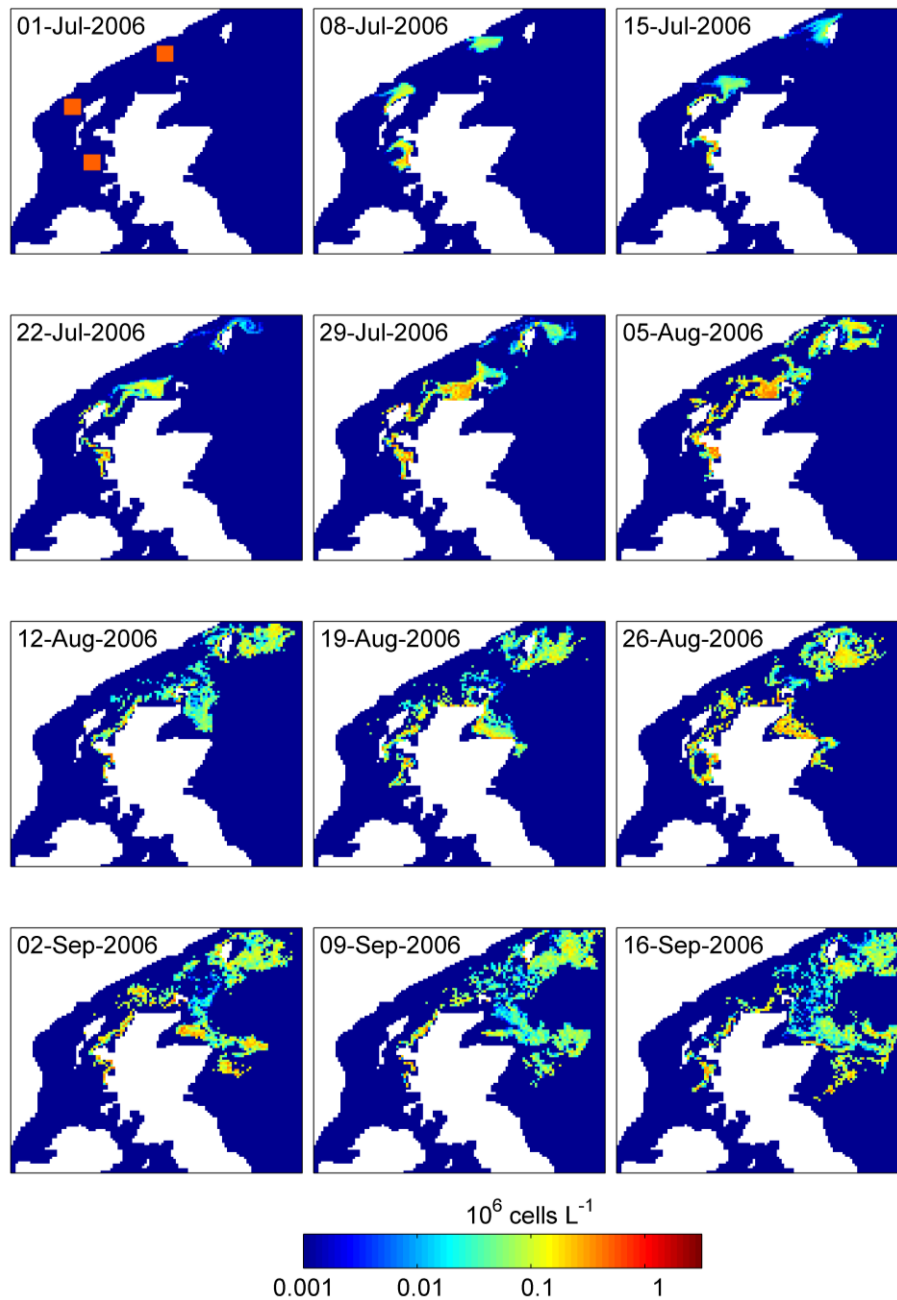
Figure 7. Model-predicted surface concentrations of *K. mikimotoi* cell density (10^6 cells L^{-1}), at weekly intervals, with the initial bloom on 1st July confined to south-western and north-western regions of the Scottish shelf and concentrations elsewhere initially set to zero. This simulation represents a multiple incursion of *K. mikimotoi* onto the shelf from the NE Atlantic.
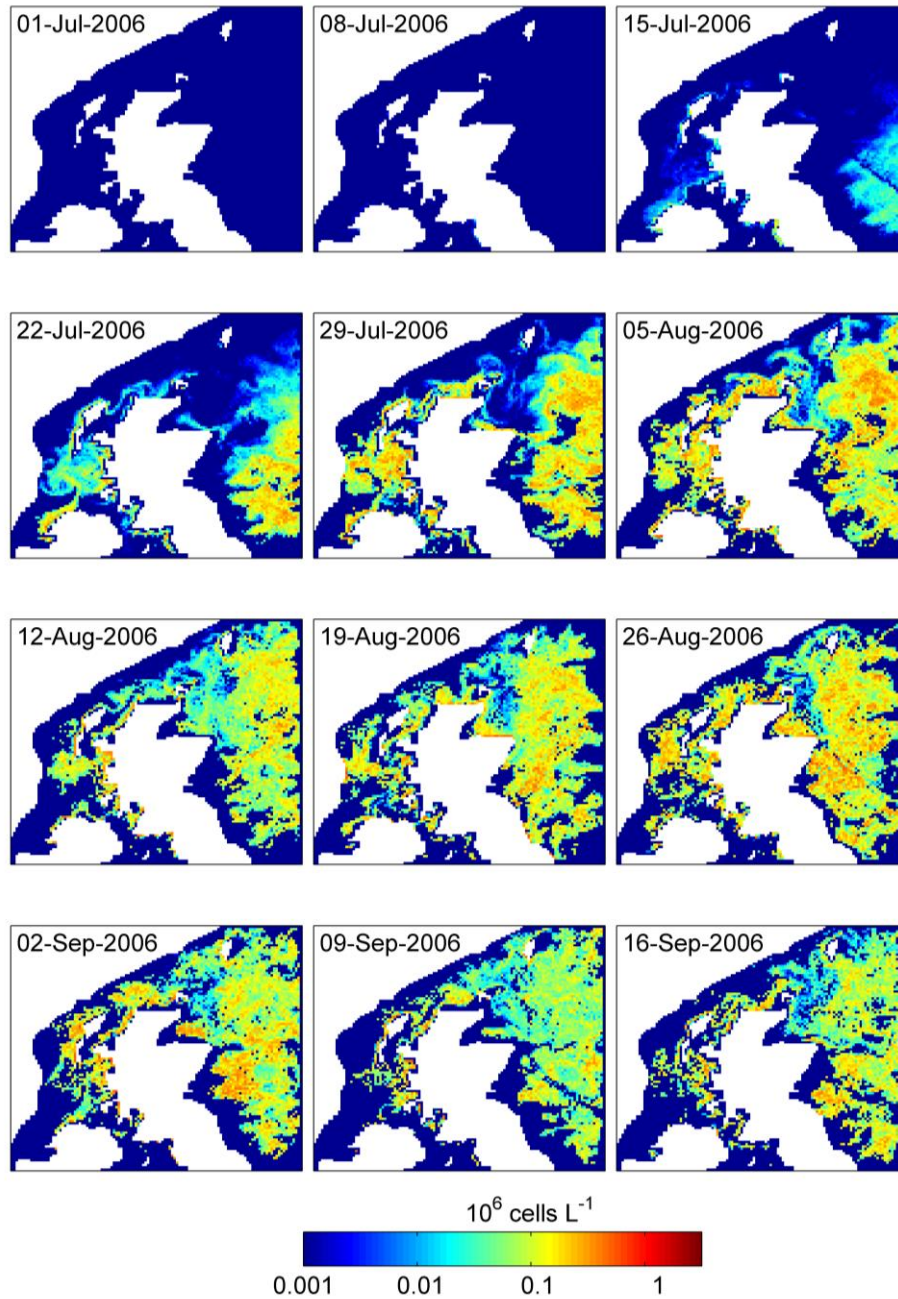
Figure 8. Model-predicted surface concentrations of *K. mikimotoi* cell density (10^6 cells L^{-1}), at weekly intervals, with the initial bloom on 1st July confined to three locations on on the Scottish shelf and concentrations elsewhere initially set to zero. This simulation represents a multiple incursion of *K. mikimotoi* onto the shelf from the NE Atlantic.

Figure 9. Model-predicted surface concentrations of *K. mikimotoi* cell density (10^6 cells L^{-1}), at weekly intervals, from the simulation with the initial distribution on 1st July specified as a uniform concentration of 56 cells L^{-1} throughout the domain.
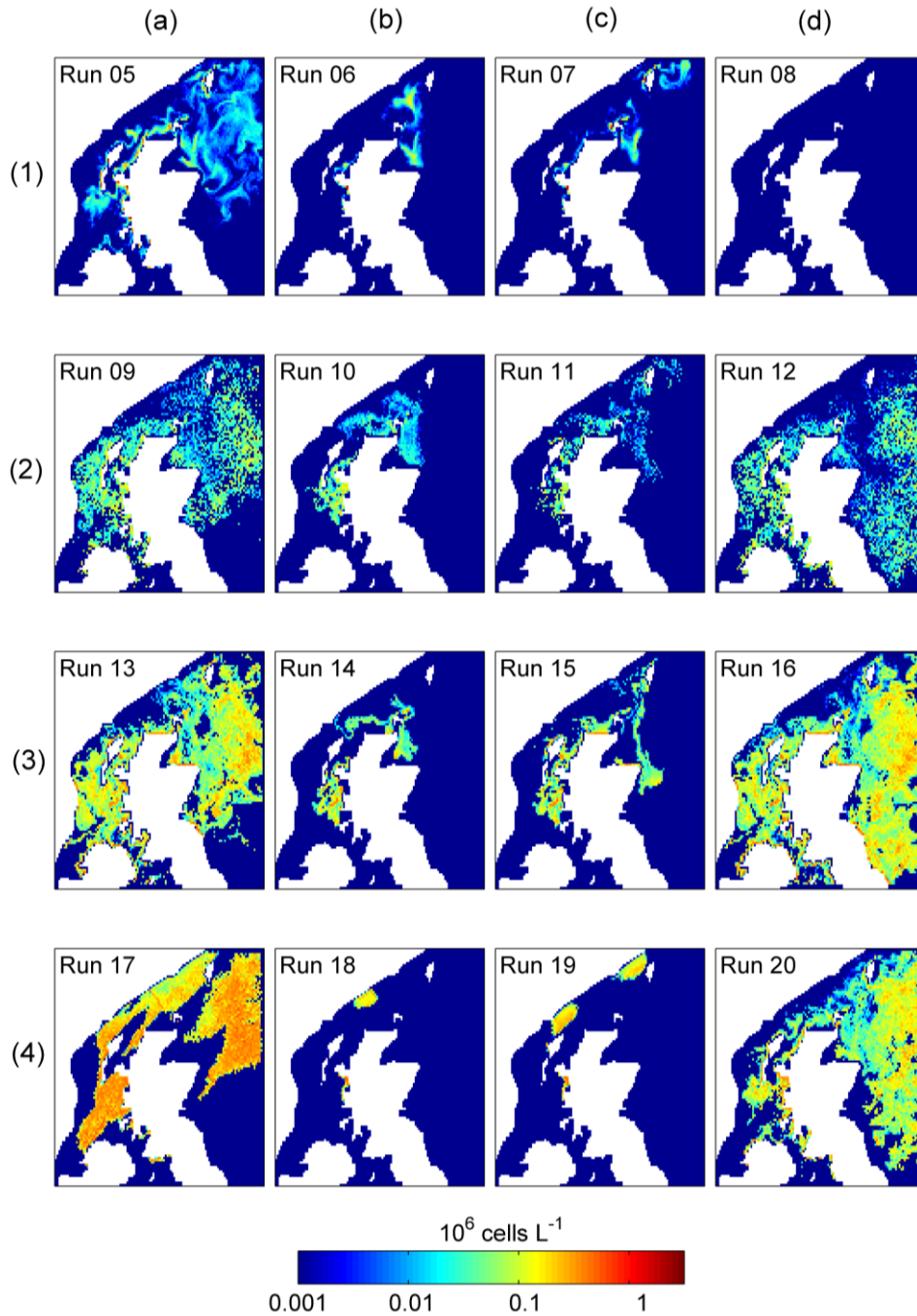
Figure 10. Model-predicted surface concentrations of *K. mikimotoi* cell density (10^6 cell L^{-1}) on 12th August 2006 for different model simulations. Run numbers for each plot refer to Table 2. Columns: (a) domain-wide initial population; (b) two-location initial population; (c) three-location initial population; (d) uniform initial population. Rows: (1) no growth or mortality; (2) no vertical migration; (3) no wind forcing; (4) zero velocity. Distributions shown in columns (a) – (d) should be compared with the results from 12th August 2006 in Figs. 6 – 9 respectively.
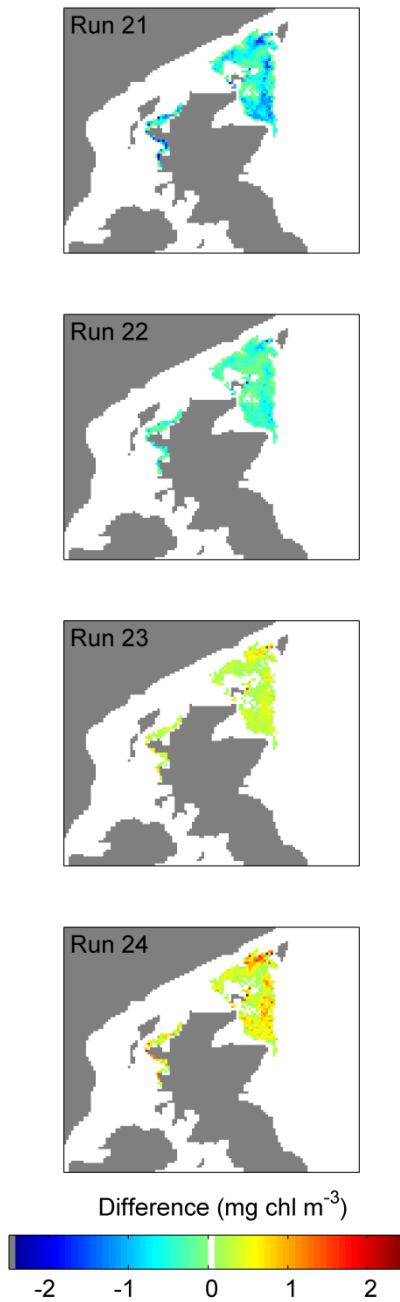
Figure 11. Difference in the modelled surface chlorophyll *a* distributions (mg m^{-3}) on 12th August 2006 between the temperature sensitivity simulations and the distribution from Run 2 (Fig. 7). In the simulations shown, the water temperatures, T, from the MRCS model were modified by fixed amounts. Run21: T = T - 1.0 °C; Run22: T = T - 0.5 °C; Run23: T = T + 0.5 °C; Run24: T = T + 1.0 °C.